Revista Geoaraguaia
ISSN:2236-9716
Barra do Garças - MT
v.9, n.2, p.1-21. Agosto 2019

MAGMATIC DIFFERENTIATION EVIDENCES AND SOURCE CHARACTERISTICS USING MINERAL CHEMISTRY IN THE TORUD INTRUSION (NORTHERN IRAN)

EVIDÊNCIAS DE DIFERENCIAÇÃO MAGMATICA E AS CARACTERÍSTICAS DE FONTE USANDO QUÍMICA MINERAL NA INTRUSÃO DE TORUD (NORTE DO IRÃ)

Abdollah Yazdi
Assistant Professor, Department of Geology, Kahnooj Branch, Islamic Azad University, Kahnooj, Iran
yazdi_mt@yahoo.com

Elham Shahhosini
Assistant Professor, Young Researchers and Elite Club, North Tehran Branch, Islamic Azad University, Tehran, Iran

Rahim Dabiri
Associate Professor, Department of Geology, Mashhad Branch, Islamic Azad University, Mashhad, Iran

Hamid Abedzadeh
Instructor, Department of Mining Engineering, Kahnooj Branch, Islamic Azad University, Kahnooj, Iran

ABSTRACT

The granitoid bodies is located 120 km north-east of Shahrood town. The area is structurally located in the north of the central Iranian zone. These activities occurred during the Upper Eocene stage. This article describes a compositional study on biotites, plagioclase of monzonites of the granite rocks of Torud area and elucidates the geotectonic and geothermobarometry conditions. The main minerals of granitoids are quartz, plagioclase, and K-feldspar. Other constituents of these rocks are biotite, amphibole, sphene, and opaque minerals. Various textures such as granular, myrmekite and graphics are observed in these rocks. Based on the geochemistry studies Plagioclase monzonite, Quartzmonzonite rocks of range anorthoclase and granite rocks are in the range of albite. Biotite compositions in the granitoid bodied depend mostly on temperature of crystallisation and oxygen fugacity (fO_2) and compositions of magmas from which they have been crystallised. The calculated Ti in biotite temperatures for the Troud granitoids are in the range of 530-900 °C. The biotite compositions used to discriminate tectonic settings of granitoids. The biotite compositions were used to discriminate the tectonic setting of the plutons. biotites granitoid rocks are the type of magmatic, rich in iron- magnesium, anorogenic alkaline and areas tensional. Based on the Major and trace element granitoid rocks different trends is show by Rb with Si and Ba with Si indicate occurrence of fractional crystallization processes (AFC). Based on the petrography, geochemistry and desert studies of the calc-alkaline, metaluminous, and series I granitoids, it can be inferred that the volcanic arcs of the

continental margin are the orogenic areas that have originated from the partial melting of crust igneous rocks. The intrusions appeared to be related to calc-alkaline orogenic suites. granitoid rocks are associated with the subduction zone neotethys.
Keywords: Plutonic Rocks; Mineral Chemistry; Torud; Iran.

INTRODUCTION

The area is located between 54˚ 30́ - 54˚ 40' longitudes and between 35˚ 15́ - 35˚ 25' latitudes, and the south of Damghan city. This area is 15 square kilometers (Figure 1). Central Iran consists of the Alborz Mountains in the north, the Zagros Mountains in the south and west, and the scattered mountains of Khorasan in the east. It includes the provinces of Esfahan, Yazd, Chahar Mahal and Bakhtiari, Markazi, Qazvin, Alborz, Tehran, Qom and Semnan of Iran. Most of the region has a warm and dry weather with a milder climate in the mountain areas. The major cities are Tehran, Esfahan, Arak, Yazd, Karaj, Qazvin, Qom, Kashan, Saveh and Shahr-e Kord.

GEOLOGY

The studied area is a part of Moaleman region (1:250.000). This area is located 120 km away from Shahrood city in north-east and comes under the central Iran zone. The northern mountain ranges of Moaleman-Torud constitute to the major part of this area. The magmatic activities had occurred in several main stages (Upper Eocene-Oligocene, Oligocene-Miocene and Pliocene) in central Iran during the Tertiary period. This area includes Moaleman-Torud in which, these activities occurred during the Upper Eocene stage. After orogenesis in Late Cretaceous, a large amount of the volcanic rocks of basalt, andesite, dacite, and rhyolite were deposited in Eocene period that were accompanied by pyroclastic and clastic sediments. This created the Karaj formation in the central Iran and Alborz.

In the studied area, equivalent deposits are called as similar-Karaj formations. The beginning of Paleozoic era was accompanied by dryness. The sediments are mainly clastic and shallow. Schist, limestone, crystalline dolomite, marble, and metamorphic sandstone constitute this collection. The beginning of Mesozoic was accompanied by the sea advancement and sedimentation in Triassic era. After tectonic stresses in the south of Anjilo fault, the cretaceous sea created an advanced transformation.

Revista Geoaraguaia
ISSN:2236-9716
Barra do Garças - MT
v.9, n.2, p.1-21. Agosto 2019

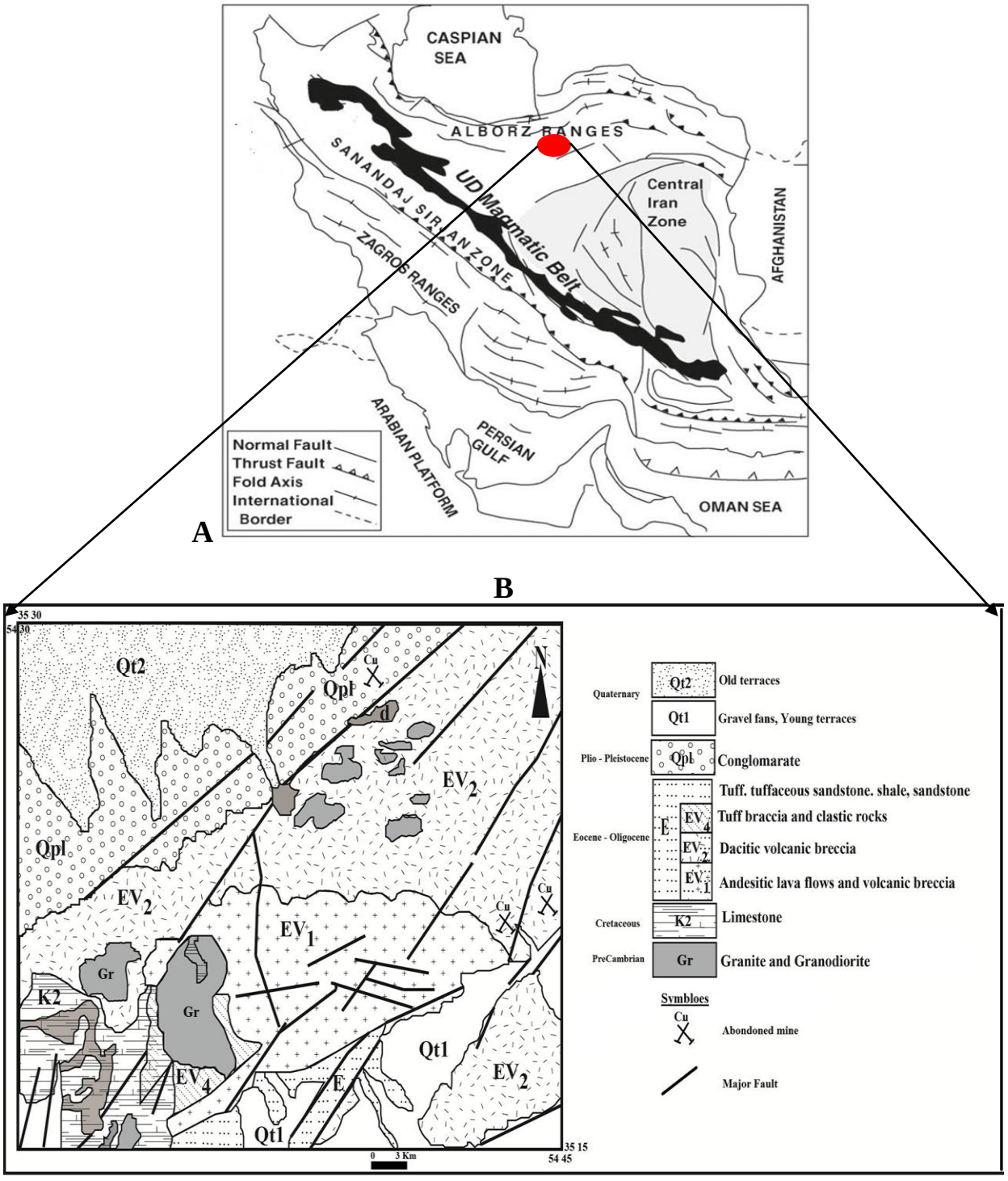

Figure 1: A: Structural subdivision map of Iran (GILE *et al.*, 2006).
B: The study area. Mapping of structural-sedimentary units and location of the study area, and geographical location of the study area of (1:250.000) Torud map

The beginning of Tertiary was accompanied by the subsidence of the bed of the sedimentary area and the sea advancement. The result was a progressing conglomeration. The volcanic-sedimentary rocks of Eocene in this area are intersected by numerous intrusive rocks. They are in the form of domes, stocks and dikes; and are existent among cretaceous carbonate rocks, older constituents, and volcanic-sedimentary rocks. The volcanic-sedimentary rocks are intersected by basic dikes, which exist in almost whole area. In this area, the structures of faults and creases have been extended from north-east to south-west (HOUSHMANDZADEH *et al.*, 1978).

ANALYTICAL METHODS

Ten rock samples including monzonite, quartz monzonite and granite were selected for analysis. The major element and some trace element analyses for all crystalline phases were performed using a CAMECA SX-50 electron microprobe (updated to SX-100 standards) at Kansaran Binalood Lab. Natural mineral standards were used for the calibration. Accelerating voltages, current and peak counting times were measured. All biotites were analysed using a focused (1 mm) 20 nA beam with an accelerating voltage of 15 kV. Feldspars were analysed using a defocused (20 mm), 10nA beam, with a 15kV accelerating voltage. To assess the precision of these analyses, standard measurements were taken during each analytical session, and averages and standard deviations were determined. Most accepted values were within deviation of the average.

DISCUSSION

Petrography

From the perspective of petrography, the granitoid rocks which have a composite of monzonite, monzodiorite, granodiorite and monzogranite of Moaleman area have changed.

The monzogranite intrusive rocks

These rocks are in the eastern side of Kouhzar village. They are seen as a large stock in the NW of the 1:100.000 map. These rocks are white and made of tiny particles. The main minerals of these rocks are plagioclase, quartz and alkaline feldspar (Figure 2A at D).

Tourmaline, seen as black spots, was created by leachate residues of granite magma differentiation, which were created by melting crust. In this area, silica and argillic alterations are also observed that include kaolinite. These rocks have a granular and porphyroid microscopic texture. Mafic minerals are mainly altered chlorite and sphene. Besides, other minerals such as plagioclase, orthoclase, and mafic minerals have also been severely altered.

Granodiorite intrusive rocks

The many of the intrusive rocks of the area are granodiorites, which intruded into the Eocene volcanic rocks. The colour of the rocks is grey and grey-green. The microscopic texture is usually granular, and the granules are medium to big in size. Sometimes, graphic, porphyroid, and granofiric textures can be observed among them. In some parts, there are enclaves, which were cooled earlier. The main minerals are plagioclase, quartz, potassium feldspar and hornblende. The minor minerals are biotite, pyroxene, apatite, sphene and opaque minerals (Figure 2C). The result of the alteration of these rocks is the formation of chlorite, epidote, sericite, sphene and clay minerals.

Monzonitic intrusive rocks

There are some large intrusive rocks in the north of Gandi village and the valley which leads to Chalou iron mine. The main part of the intrusive rocks of this area has been made of monzonite, quartzmonzonite and quartzmonzodiorite, which have intruded into Eocene volcanic rocks and limes belonging to Cretaceous. The result of the intrusion of these rocks is skarn formation at the point of contact with lime.

Based on the field observations, garnet and epidote are created, and the limestone has recrystalised and turned into white. In addition to iron mineralisation, copper (malachite and azurite) and lead mineralisation is also observed in this area, although to a lesser extent. In contrast to 1:100.000 map, the rocks of this area have mainly been made of intrusive rocks. The colour of the intrusive rocks in normal sizes is grey and grey-green.

In terms of texture, the granules are medium to big in size. In normal sizes, feldspar minerals, quartz and ferromagnesian minerals (hornblende) can also be observed. At a microscopic scale, the texture is granular. Sometimes graphic, porphyroid and poikilitic textures

are also observed. In some parts, they have a large amount of mafic micro-granular enclaves. The main minerals are plagioclase, quartz, potassium feldspar, and hornblende. The minor minerals are biotite, pyroxene, apatite, sphene, and opaque minerals (Figure 2B). The minerals resulted from the alteration of rocks are chlorite, epidote, sericite, sphene and clay minerals.

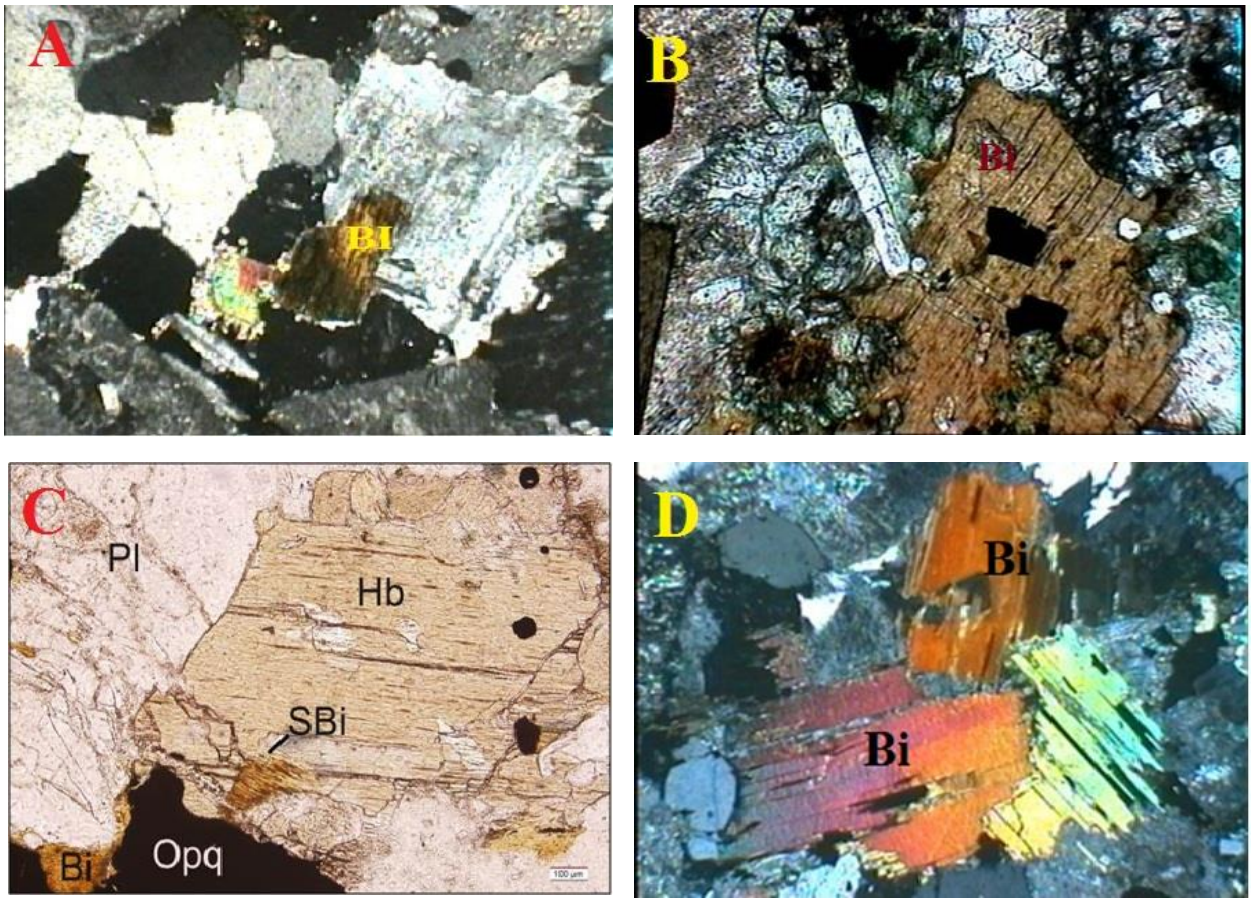

Figure 2: A: In microscopic image sequence in which minerals crystallize first, biotite, and plagioclase, K-feldspar and quartz have crystallized at the end XPL) (100X, Field Lengh: 2.2mm);
B: In microscopic image of the form inclusions in apatite-bearing biotites in quartz monzodiorite (XPL) (100X, Field Lengh: 2.2mm);
C: image of biotite metasomatism green hornblende granodiorite stone (PPL). (100X, Field Lengh: 2.2mm);
D: microscope image showing the biotite in granitic rocks (XPL) (100X, Field Lengh: 2.2mm).

Crystallisation conditions of biotite

The major elemental compositions and structural formulas of the biotites and the compositions of K-feldspars are given in Tables 2 and 3. A number of authors Verhoogen

(1962a; 1962b), Taylor (1964), Buddington and Lindsley (1964) and Albuquerque (1973) have suggested that Ti^{4+}, $Al^{[6]}$ and Fe^{3+} are the most important elements to be considered in the understanding of the petrogenetic problems for granitic rocks. Looking at the diagram Deer *et al.* (1962), Spear (1984) samples were within the biotite (Figure 4). The compositions of Ti^{4+} and Fe^{3+} depend mostly on temperature of crystallisation and oxygen fugacity (fO_2). Gorbatschev (1968) proposed that the content of Ti and AI vx in the biotite is mainly regulated by dimensional requirements of the octahedral and tetrahedral layers. As a considerable amount of Al enters the tetrahedral sites replacing Si, Ti can enter more readily the octahedral sites and this offsets the temperature effect which would tend to restrict the amount of Ti entering the structure of biotite. There is therefore an inverse correlation between Si in biotite and in the host rock, while both Aliv and Alvi increase with increasing Si of the host rock (ALBUQUERQUE, 1973).

Previous works (WONES and EUGSTER, 1965; DODGE *et al.*, 1969; ALBUQUERQUE, 1973; BARRIERE and COTTON, 1979; NEIVA, 1981) have pointed out that the Fe^{3+} contents and Fetot/ (Feo_t + Mg) ratios provide at least relative information about the oxygen fugacity during the crystallisation. According to Wones and Eugster (1965) water fugacity (fH_2O) can be calculated if the oxygen fugacity (fO_2), temperature and pressure of equilibration for a mineral assemblage of biotite (Mg-rich) + K-feldspar + magnetite have been determined.

The major and trace element contents and modal compositions of the whole rocks have been used to provide information on the tectonic settings of igneous rocks by several authors (PEARCE and CANN, 1973; FLOYD and WINCHESTER, 1975; DEBON and LE FORT, 1982; PEARCE *et al.*, 1984). The biotite compositions can also be used to discriminate tectonic settings of granitoids. When the biotites plotted on Al_2O_3-FeOt-MgO and Al_2O_3-MgO plots (Figure 5C and D), as postulated by Abdel-Rahman (1994), fall in the field of calc-alkaline to slightly alkaline orogenic suites.

According to Deering *et al.* (2012), the insensitivity of hydrogen isotope fractionation to magma differentiation ensures that mineral δD reflects the original fluid composition even as magma evolution progresses from primitive basalt to the most evolved silicic magma. Therefore, δD values from hydrous minerals like biotite could be a petrogenetic signiture for determination of magma origin.

Determination of mineral

The mineral species were identified on the basis of the obtained results and diagrams.

A. Plot Or-Ab-A long Deer *et al.* (1991) was used to determine plagioclase igneous rocks (Figure 3).

B. To specify the type, the spreadsheet (spreadsheet is a sheet of paper that shows accounting or other data in rows and columns; a spreadsheet is also a computer application program that simulates a physical spreadsheet by capturing, displaying, and manipulating data arranged in rows and columns. The spreadsheet is one of the most popular uses of the personal computer) of plagioclase using two types of minerals have been calculated and given below (Table 1).

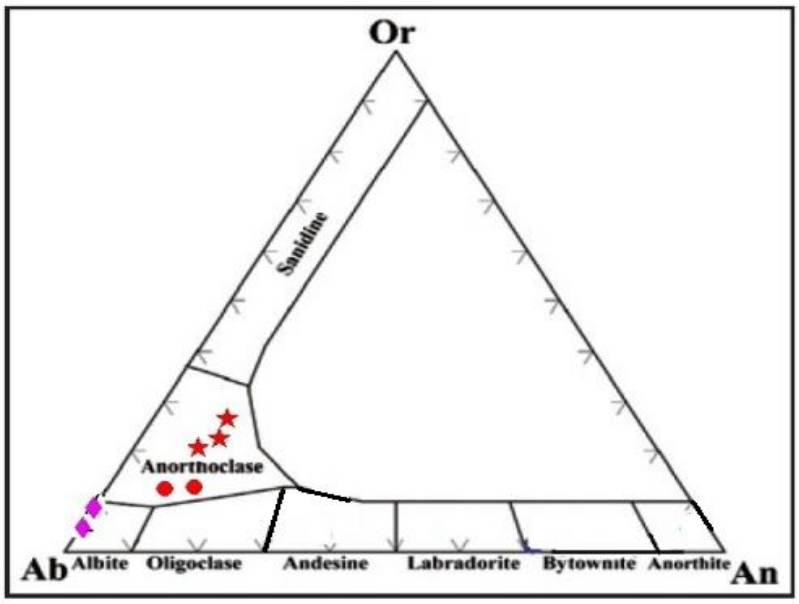

Figure 3: The composition of igneous rocks TORUD feldspars Deer *et al.* (1991)

● Monzonitic ✦ Quartzmonzonite ◆ Granites

Table 1: **Determination of plagioclase on the Spreadsheet**

	Or	Ab	An	Sum
E68-GR-1	0.960	98.60	0.44	100
E68-GR-2	5.59	93.53	0.86	100
E28-QMO-1	56.269	37.12	6.61	100
E28- QMO-2	55.14	36.20	8.65	100
E113-MO-1	58.18	38.15	3.66	100
E113-MO-2	51.90	40.80	7.28	100
E94-GA-1	57.20	15.35	27.44	100
E94-GA-2	68.92	16.51	14.55	100
E119-GA-1	61.29	16.33	22.37	100
E119-GA-2	61.23	16.33	22.42	100

Table 2: **Analysis of the biotite zone plutonic rocks TORUD**

Sample	Gd-BI1	Gd-BI2	Gd-BI3	MG-BI4	Gd-BI5	MG-BI6	MG-BI7	G-BI8
SiO_2	34.79	33.53	34.9	35.13	34.94	36.59	34.25	33.6
Al_2O_3	19.92	19.35	23	19.81	20.35	15	18.85	18.2
MgO	8.66	8.5	7.55	8.28	8.52	11.71	7.05	5.77
FeO	21.09	21.46	18.62	20.84	20.67	14.97	18.96	20.23
TiO_2	1.83	1.89	1.45	1.64	1.37	3.79	4.69	4.96
MnO	0.3	0.26	0.32	0.24	0.29	3.51	2.34	2.24
Na_2O	0.25	0.27	0.3	0.3	0.29	0.04	0	0.03
K_2O	8.08	7.43	7.04	8.07	7.79	0.12	0.2	0.06
Cr_2O_3	0.06	0.07	0.06	0.06	0.09	8.55	8.57	8.49
NIO	0.07	0.1	0	0.05	0.01	0.11	0.03	0.08
TOTAL	95.07	93.09	93.29	94.45	94.46	94.58	95.2	94.2
Si	2.66	2.63	2.65	2.7	2.68	2.79	2.66	2.67
ALIV	1.34	1.37	1.35	1.3	1.32	1.21	1.34	1.33
ALVI	0.46	0.42	0.72	0.49	0.51	0.14	0.39	0.37
Mg	0.99	1.01	0.86	0.95	0.97	1.33	0.82	0.68
Fe	1.35	1.41	1.18	1.34	1.32	1.2	1.54	1.67
Ti	0.11	0.11	0.08	0.09	0.08	0.2	0.14	0.13
Mn	0.01	0.01	0.01	0.01	0.01	0.01	0.01	0.01
Cr	0	0	0	0	0	0	0	0
Na	0.04	0.04	0.04	0.04	0.04	0.02	0.03	0.01
K	0.79	0.74	0.68	0.79	0.76	0.84	0.85	0.86
TOTAL	7.74	7.75	7.59	7.72	7.72	7.75	7.78	7.75

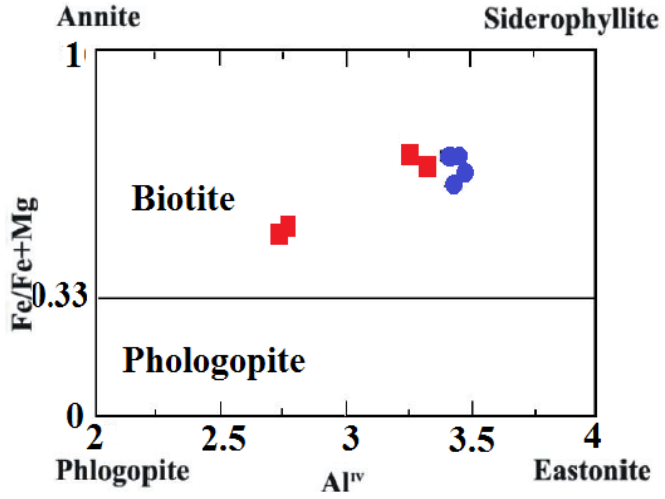

Figure 4: Compositional Classification of Biotite Deer *et al.* (1962); Spear (1984).
Granites and monzogranites: ■ Granodiorites: ●

Table 3: **Analysis of the plagioclase and K-feldspar plutonic rocks TORUD area**

	E94-Ga-1	E94-Ga-2	E119-GA-119-1	E119-GA-119-2	E113-mo-1	E113-mo-2
Element	**Mass%**	**Mass%**	**Mass%**	**Mass%**	**Mass%**	**Mass%**
Na_2O	7.01	5.44	6.85	6.28	6.2	4.56
Al_2O_3	21.57	22.01	20.66	20.7	24.57	23.72
MgO	0.4	0.45	0.4	0.4	0.22	0
CaO	3.36	2.92	3.6	3.35	8.13	7.17
P_2O_5	0	0.24	0	0	0	0.12
Fe_2O_3	0.56	1.03	1.02	1.25	0.45	0.51
SiO_2	65.49	65	64.75	65.15	59.83	63.08
K_2O	1.48	2.61	2.5	2.3	0.39	0.64
Cr_2O_3	0	0	0	0	0	0
Rb_2O	0.01	0.01	0.01	0.01	0.01	0
ZrO_2	0.01	0.01	0	0	0.01	0.01
SO_3	0.03	0.01	0.01	0	0.02	0.05
SrO	0.08	0.11	0	0	0.14	0.15
MnO_2	0	0.05	1	0.04	0	0
TiO_2	0	0.08	0.08	0.5	0.01	0
As_2O_5	0	0	0	0	0	0
ZnO	0	0	0	0	0.02	0
TOTAL	100	99.97	100.88	99.98	100.494	100.01
SiO_2	2.60	2.62	2.59	2.61	2.40	2.53
TiO_2	0.00	0.00	0.00	0.02	0.00	0.00
Al_2O_3	1.18	1.15	1.10	1.10	1.31	1.27
Cr	0.00	0.00	0.00	0.00	0.00	0.00

FeO	0.08	0.05	0.08	0.10	0.04	0.04
MnO	0.00	0.00	0.03	0.00	0.00	0.00
MgO	0.04	0.03	0.29	0.03	0.02	0.00
CaO	0.23	0.27	1.09	0.27	0.65	0.58
Na_2O	0.87	1.12	0.40	1.01	0.99	0.73
K_2O	0.42	0.24	0.00	0.37	0.06	0.10
TOTAL	5.44	5.48	5.60	5.51	5.47	5.25
Or	57.203	68.928	61.30	61.238	58.189	51.907
Ab	15.352	16.519	16.33	16.333	38.151	40.808
An	27.445	14.553	22.37	22.428	3.66	7.285

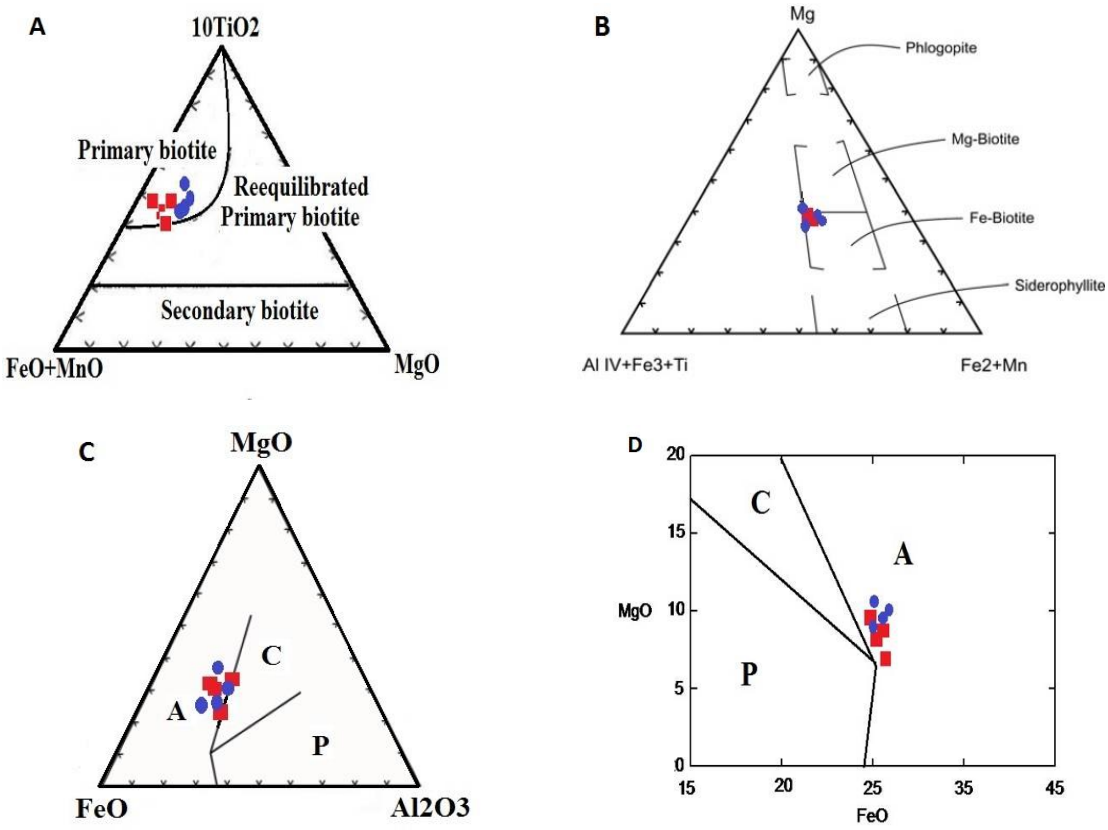

Figure 5: A: Diagram adapted from Nachite *et al.* (2005);
B: Relation between octahedral cations of the studied biotite (after Foster, 1960);
C and D: The biotite compositions were used to discriminate tectonic settings of granitoids (Abdel-Rahman, 1994);
A: Biotite in anorogenic alkaline and areas tensional;
P: Peraluminous rocks and environments interact;
C: Calc-alkaline rocks and subduction zones

CRYSTALLISATION PROCESSES

Major and trace element concentrations of the analysed rocks are listed in Tables 4 and 5. Herein, some LILE and HFSE vs. silica variograms with fractionation trends of some selected major rock forming minerals as conducted by Koprubas and Aldanmaz (2004) in some west Anatolian granitoids (Figure 6) are presented. For example, slightly decreasing rubidium content with an increase in silica can result from biotite-bearing fractionation in the rock samples (Figure 6a). On the contrary, slightly increasing Rb with increasing silica may indicate occurrence of AFC processes in the rock samples (Figure 6a). Barium vs. silica variograms show two different trends that are consistent with clinopyroxene fractionation in the granitoid units, and with plagioclase fractionation Torud batholith (Figure 6b). A strontium vs. silica diagram clearly reveals that biotite fractionation had affected all the subunits of the composite Torud batholith (Figure 6c).

Table 4. **Major element compositions of rocks from the Torud area**

Sampl.	E70-GA	E77-MG	E72- QM	E82-QM	E91-QM	E118-QM	E73- GR	E99-GA
SiO_2	62.95	63.92	65.55	64.27	63.29	60.61	62.24	64.59
Al_2O_3	19.14	17.53	18.23	16.14	15.98	15.77	17.8	15.51
FeO	4.07	6.07	4.23	4.66	4.85	6.33	5.97	4.5
CaO	3.23	1.55	0.41	2.94	3.84	4.81	2.98	3.88
MgO	3.43	2.58	2.36	2.84	3.42	3.48	2.57	2.86
Na_2O	4.06	2.89	2.97	3.25	3.53	3.07	3.09	3.16
K_2O	1.66	4.23	5.22	4.67	3.94	4.5	4.12	4.39
P_2O_5	0.52	0.31	0.2	0.3	0.42	0.51	0.31	0.41
MnO	0.1	0.1	0.1	0.1	0.1	0.2	0.1	0.1
TiO_2	0.73	0.72	0.61	0.61	0.42	0.51	0.72	0.51
SrO	0.1	0.1	0.1	0.2	0.21	0.2	0.1	0.1
MG	427.2752	300.5041	291.792	344.9442	412.5155	402.9763	300.0486	349.5556
ASI	1.00	0.97	0.96	1.19	1.23	1.34	1.12	1.24

GR: Granodiorite QM: Quartzmonzonite GA: Granite MG: Monzogranite

The variation in a plot of yttrium vs. silica content represents two different trends similar to that of rubidium. The rock samples are more consistent with an amphibole-bearing fractionation (Figure 6d). It is noted here that the rock samples from the Torud quartz monzonite have a transitional character in terms of the silica content. HCl/HF is typically positive in metaluminous plutons, whereas HCl/HF is typically negative in peraluminous plutons; H2O/HF

is generally positive overall, but particularly in the metaluminous plutons. In summary, apatite appears to have equilibrated with an earlier HCl- and H2O-rich magmatic fluid and biotite appears to have equilibrated with a later similarly HCl-rich, but particularly H2O-rich magmatic fluid (RASMUSSEN and MORTENSEN, 2013). The H2O/HF enrichment in the magmatic volatiles determined from biotite in the magmas most closely associated with mineralization (RASMUSSEN and MORTENSEN, 2013).

Table 5: **Trace element and REE concentrations of rocks from the Torud area**

Sampl.	E70	E77	E72	E82	E91	E118	E73	E99	E83
Be	1.81	2.06	1.69	2.53	1.99	2.65	2.06	2.78	1.3
Bi	0.5	0.58	0.5	0.5	0.5	0.5	0.57	0.5	0.5
Ce	51.55	55.25	28.34	55.14	30.45	41.85	58.34	58.06	38.82
Co	10.95	20.03	23.24	13.82	13.6	12.63	20.02	9.56	17.62
Cr	34.95	73.25	94.84	96.06	67.04	76.12	82.78	73.25	64.64
Cu	3.33	31.21	130	56.05	39.5	56.37	68.21	38.45	80.61
Dy	6.65	3.96	2.42	7.57	0.97	0.08	7.51	0.08	2.99
Er	1.56	1.31	0.66	2.24	1.7	1.39	2.38	2.07	2.39
Eu	1.44	1.21	0.45	1	0.74	1.17	1	1.96	1
Ga	23.22	21.54	27.95	25.43	13.23	25.24	20.73	22.93	19.36
Gd	3.8	5.1	3.43	5.22	3.43	4.14	5.11	4.82	4.9
Ge	0.9	1.91	1.18	1.19	1.26	1.04	1.7	0.77	1.42
Hf	5.33	8.91	5.89	8.06	5.66	7.13	7.72	9.5	8.87
Ho	0.48	0.61	0.3	0.62	0.4	0.62	0.62	0.75	0.61
La	27.07	27.94	12.89	29.3	18.68	25.13	30.89	29.43	19.99
Li	29.71	25.01	18.58	11.49	9.5	10.29	25.76	9.46	12.19
Lu	0.23	0.37	0.24	0.35	0.21	0.31	0.33	0.41	0.8
Mn	285	605	354	445	684	865	477	1459	601
Mo	15.73	6.39	6.94	25.61	25.75	34.78	11.06	7.48	7.88
Nb	20.02	23.26	19.66	25.59	14.19	17.58	26.16	23.42	24.3
Nd	30.12	24.39	15.37	24.99	19.43	28.48	54.56	32.84	18.81
Ni	16.9	39.61	55.66	28.41	29.29	27.72	43.51	25.59	19.26
P	1277	825	567	883	1072	1082	803	1567	1243
Pb	4.82	16.83	11.21	22.83	45.65	17.79	16.49	21.83	15.9
Pr	8.34	8	5.66	10.14	6.37	12.5	8.38	6.76	5.58
Rb	116	114	44.54	134	173	223	85.57	238	157
Sc	11.13	11.33	9.14	10.2	8.27	10.62	9.14	14.39	14.97
Se	0.08	0.12	0.11	0.19	0.13	0.05	0.08	0.06	0.06
Sm	4.69	4.66	2.21	4.71	2.53	3.6	5.3	4.87	3.64
Sn	1.97	3.02	2.09	2.9	1.91	2.64	2.79	3.22	3.09
Sr	397	392	158	435	516	766	295	822	488
Ta	1.23	2.74	1.77	2.63	1.53	1.78	3.11	1.62	2.85
Te	0.18	0.28	0.21	0.27	0.19	0.24	0.26	0.31	0.29
Th	9.71	14.49	9.26	17.41	9.49	12.87	15.7	16.51	14.46
U	2.71	5.01	3.61	3.42	3.32	3.1	5.22	2.76	4.4
V	144	137	110	130	107	136	140	176	186

Y	14.93	16.49	7.34	20.65	9.49	12.68	20.39	16.37	18.16
Yb	1.47	1.78	1.08	2.23	1.1	1.39	2.09	1.9	2.04
Zn	23.95	20.14	23.56	25.06	56.54	50.45	31.66	63.56	25.06
Zr	40.48	13.12	9.46	43.84	54.66	44.91	13.12	22.98	38.7

Results studies Bray *et al.* (2014) show that the concentration of protons consumed by biotite, during the titration series, increases with decreasing pH. The minimum proton consumption occurs at pH-10, consistent with the immersion pH (pHimm). The total amount of metals released from dissolution and metal–proton exchange reactions increases with decreasing pH.

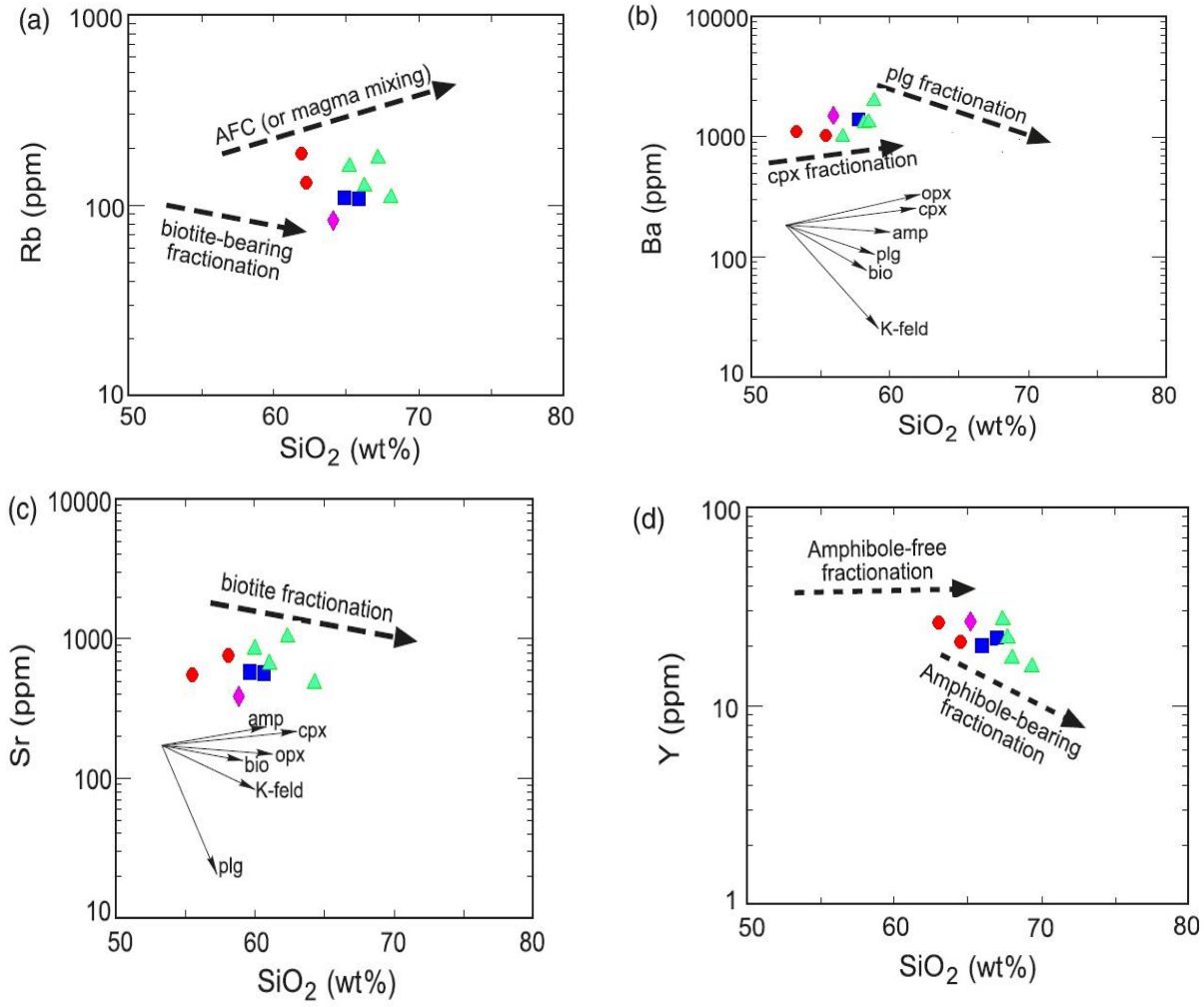

Figure 6: Rb, Ba, Sr and Y vs. silica semi-logarithmic variation diagrams of granites from the composite Torud batholith.The arrows, adapted from Koprubas and Aldanmaz (2004), indicate theoretical Rayleigh fractionation vectors modelled for crystallisation of individual mineral phases.

The Ti-content of biotite can be used for temperature calculations using Henry *et al.* (2005) formula. Precise values were estimated based on Henry *et al.* (2005) equation T = {(lnTi–a–c(XMg)3)/b}0.333, in which XMg is Mg/(Mg + Fe), a = -2.3594, b = 4.6482-10^{-9} and c = -1.7283], which were calibrated in the ranges of XMg = 0.425–0.525, Ti = 0.08-0.2 apfu and T = 480-800°C. The calculated Ti-inbiotite temperatures for the Troud granitoids are in the range of 530-900 °C.

SOURCE CHARACTERISTICS

Chemically, the crustal source for the investigated granitoids is deduced from their Nb/Y versus Rb/Y data (Figure 7a). The granitoids in the study area have predominantly low Rb/Nb values (0.3-3.0) and the plot is similar to that for the lower crust values (RUDNICK and FOUNTAIN, 1995) (Figure 7a). High concentrations of CaO, MgO and FeOt and low K_2O/Na_2O values indicated the source of the investigated rocks as metabasites. To constrain the source material, these minerals were plotted in the partial melts from the metabasaltic source field diagram as proposed by Altherr and Siebel (2002) (Figure 7b-d).

The heat required for the partial melting of the crustal rocks might have been supplied from two possible sources. First one was the upwelling of mantle plume and advective heating of the crust by the deep-seated magma chambers. This could occur in an extensional system with lithospheric thinning (breaking-off of a downward oceanic slab) or might be related to the delaminating events in the area (GHASEMI and TALBOT, 2006). Such a model requires crystallisation of an unreasonably large volume of mafic magma generated after the cessation of subduction and crustal thickening, which is in disagreement with the scarcity of the exposed mafic suites in the study area and so is ruled out on the basis of field and lithological evidence in the Torud area. The second source of the heat required for partial melting of the crust was provided by the continental collision causing crustal thickening (AGARD *et al.*, 2005). This possibility seems to be responsible for the generation of the metaluminous granitoids in the Torud area. The ultimate nature of the crustal materials involved and melting conditions were the significant factors that caused formation of the collisional sub-alkaline granitoids in the study area.

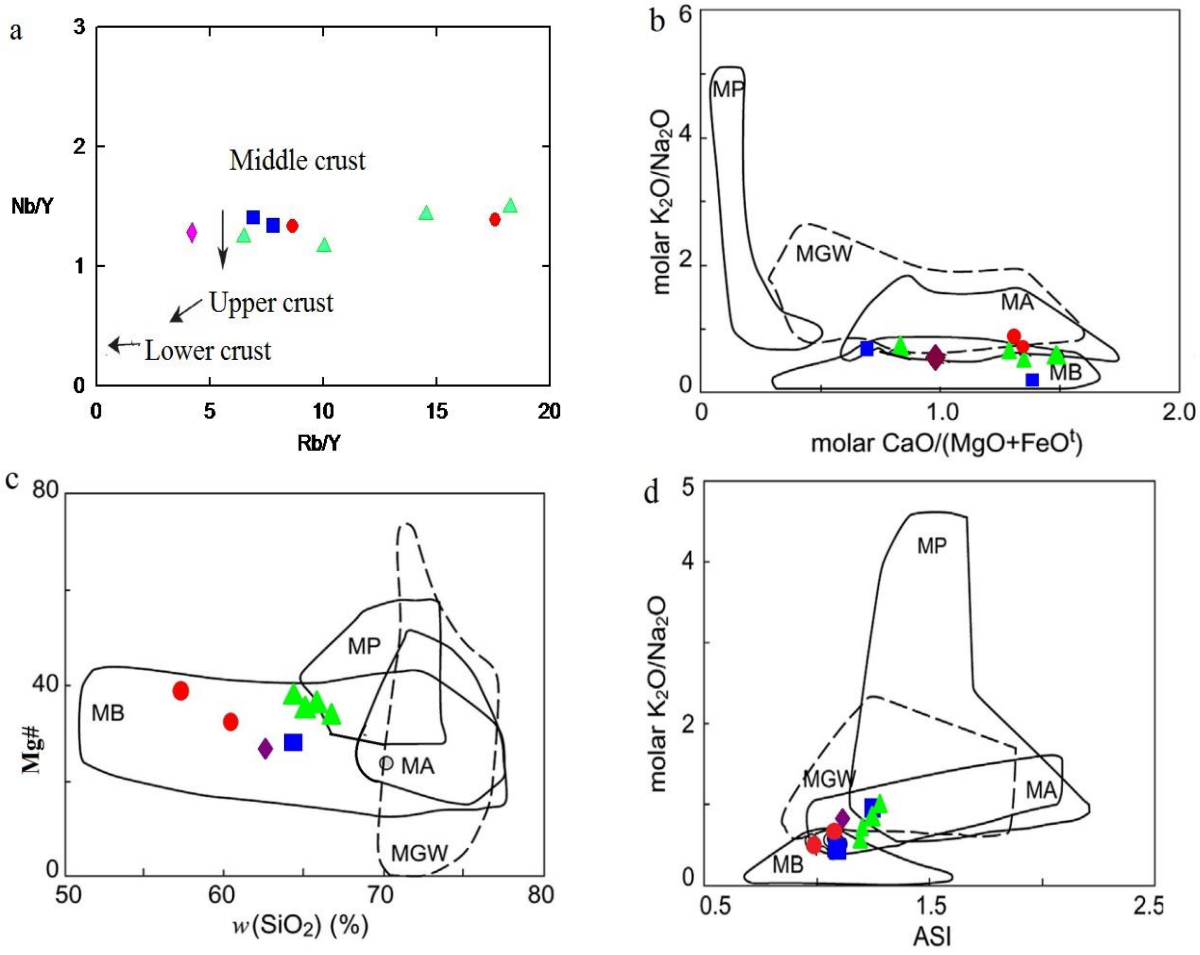

MA: meta andesite MB: meta basalt MP: meta pelites MGW: metagreywacke

Figure 7. a: Nb/Y vs. Rb/Y diagram for the Torud granitoids. The lower and middle crustal compositions are adapted from Rudnick & Fountain (1995), and the upper crustal compositions are adapted from Taylor and McLennan (1985);
b at d: According to Altherr and Siebel (2002), high concentrations of CaO and low K_2O/Na_2O ratio classify parental rocks as metabasalts. The fields on the diagram are chemical composition of melts from experimental studies of dehydration melting.
Data sources: Vielzeuf and Holloway (1988); Patin˜o Douce and Johnston (1991); Rapp *et al.* (1991); Gardien *et al.* (1995); Rapp (1995); Rapp and Watson (1995); Patin˜o Douce and Beard (1995,1996); Stevens *et al.* (1997); Skjerlie and Johnston (1996); Patin˜o Douce (1997); Patin˜o Douce and McCarthy (1998).

Melting experiments on basalts demonstrated that H_2O-saturated melting occurs between 750 °C and 800 °C at 5 kbar (HELZ, 1976). Rapp (1995) stated that melts formed by dehydration melting of amphibolites are increasingly metaluminous beyond the amphiboleout boundary. Studies of Jung *et al.* (2002), Sale *et al.* (2002) and Suda (2004) indicate that dehydration melting of amphibolites at temperatures of 900-1100 °C produces 10-60% mafic magma (SiO_2 ~50 wt%)

to form tonalite, depending on bulk composition. Based on the experimental data, it can be inferred that the production of magma with compositions analogous to that of the Torud granitoids took place under dehydration melting conditions due to hornblende breakdown in amphibolites at a temperature of 900°C and a pressure range of 5-10 kbar (WOLF and WYLLIE, 1991; WYLLIE and WOLF, 1993; RUSHMER, 1991). Considering field evidence and analogous geochemical characteristics and *P-T* relations the granitoids, it seems that the melt which originated from the partial melting of metabasites might have accumulated and the granitoids of the Torud area had been formed from this melt.

CONCLUSIONS

- The Torud granitoidic rocks are in the north of Central Iranian micro-continent.
- Tectonically, the rocks formed in a continental volcanic arc setting due to subduction of Neotethys oceanic crust beneath the Central Iran plate.
- Torud granites are composed of various granitic rocks including quartz monzonite, monzogranite, granodiorite and monzonite. They are subalkaline, calcalkaline, peraluminous and their characteristics resemble those of I-type granites.
- According to the diagram the plagioclase monzonite, quartzmonzonite rocks of range anorthoclase and granite rocks are in the range of albite.
- According to the analysis of microprobe biotites granitoid rocks, they are the type of magmatic, rich in iron- magnesium, anorogenic alkaline and areas tensional.
- Biotite compositions depend largely upon the nature of magmas from which they have been crystallised. This demonstrated that the plutons have typical arc related calc-alkaline to slightly alkaline character.
- An ascending linear pattern is indicated by some LILE and HFSE vs. silica variograms to the occurrence of fractional crystallization processes.
- All these characteristics, combined with low Al_2O_3/ (FeO + MgO + TiO_2) and (Na_2O +K_2O)/ (FeO + MgO + TiO_2) ratios and high Mg values, suggest an origin through dehydration melting of alkaline mafic of lower crustal source rocks.

REFERENCES

ABDEL-RAHMAN, A. Nature of Biotites from Alkaline, Calc-alkaline, and Peraluminous Magmas. **Journal of Petrology**. n. 35. v. 2. 1994. p. 525- 541.

ALBUQUERQUEC, C. A. R. Geochemistry of biotites from granitic rocks, Northern Portugal. **Bull. Geol. Sot. Amer**. n. 37. 1973. p. 1779-1802.

ALTHERR, R.; SIEBEL, W. I-type plutonism in a continental back-arc setting: Miocene granitoids and monzonites from the central Aegean Sea, Greece. **Contributions to Mineralogy and Petrology**. n.143. 2002. p. 397- 415.

AGARD, P.; OMRANI, J.; JOLIVET, L.; MOUTHEREAU, F. Convergence history across Zagros (Iran): constraints from collisional and earlier deformation. **International Journal of Earth Sciences**. n. 94. 2005. p. 401-419.

BRAY. A. W.; BENNING. L. G.; BONNEVILLE. S.; OELKERS. E. H. Biotite surface chemistry as a function of aqueous fluid composition. **Journal of Geochimica et Cosmochimica Acta**. n. 128. 2014. p.58-70.

BARRIERE, M.; COTTON, J. Biotites and associated minerals as markers of magmatic fractionation and deuteric equilibration in granites. **Contrib Mineral Petrol**. n. 70. 1979. p.183-192.

BUDDINGTON, A. F.; LINDSLEY, D. H. Iron-titanium oxide minerals and synthetic equivalents. **Journal of Petrology**. n. 5. 1964. p. 310-357.

DEBON, F.; LE FORT, P. A chemical-mineralogical classification of common plutonic rocks and associations. Trans. R. **Soc Edinb Earth Sci**. n. 73. 1983. p.135-149.

DEER, W. A.; HOWIE, R. A.; ZUSSMAN, J. **Rock-forming minerals**. v. 3. Sheet silicates longman. London. 1962.

DEER, W. A.; HOWIE, R. A.; ZUSSMAN, J. **An introduction to rock forming minerals**. 1991. 528p.

DEERING, C. D.; HORTON, T. W.; GRAVLEY, D.M.; COLE, J. W. Hornblende, cummingtonite, and biotite hydrogen isotopes: direct evidence of slab-derived fluid flux in silicic magmas of the Taupo Volcanic Zone, New Zealand. **Journal of Volcanology and Geothermal Research**. n. 233-234. 2012. p. 27–36.

DODGE, F. C. W.; SMITH, V. C.; MAYS, R. E. Biotites from granitic rocks of the Central Sierra Nevada Batholith, California. **Journal of Petrology**. n.10. 1969. p. 250-271.

FLOYD, P. A.; WINCHESTER, J. A. Magma type and tectonic setting discrimination using immobile elements. **Earth Planet Sci Let**. n. 27. 1975. p. 211-218.

FOSTER, M. D. Interpretation of the composition of trioctahedral micas. **US Geological Survey Prof**. v. 354B. 1960. p.1-49.

GILE, H. A.; BONI, M.; BALSSONE, G.; ALLEN, C. R.; BANKS, D.; MOORE, F. Marble-hosted sulfide ores in the Angouran Zn-(Pb-Ag) deposit, NW Iran: interaction of sedimentary brines with a metamorphic core complex. **Mineralium Deposita**. n. 41. 2006. p.1-16.

GHASEMI, A.; TALBOT, C. J. A new tectonic scenario for the Sanandaj–Sirjan Zone (Iran). **Journal of Asian Earth Sciences**. n. 26. 2006. p. 683-693.

GARDIEN, V.; THOMPSON, A. B.; GRUJIC, D.; ULMER, P. Experimental meltingof biotite + plagioclase + quartz ± muscovite assemblages and implications for crustal melting. **Journal of Geophys Res**. n.100. 1995. p.1581-1559.

GORBATSCHEV, R. **Distribution of elements between cordierite, biotite, and garnet**. Miner Abh. n. 110. 1968. p.57-80.

HELZ, R. T. Phase relations of basalts in their melting ranges at PH2O=5 kb. Part II. Melt compositions. **Journal of Petrology**. n. 17. 1976. p.139-193.

HENRY, D. J.; GUIDOTTI, C. V.; THOMSON, J. A. The Ti-saturation surface for low-tomedium pressure metapelitic biotite: implications for Geothermometry and Tisubstitution mechanisms. **Am. Mineral**. n. 90. 2005. p.316-328.

HOUSHMANDZADEH, A. S.; ALAVI, M.; HAGHIPOUR, M. Geological evolution of the phenomenon TORUD (from the Precambrian to the present Covenant). **Geological Survey**. 1978. 138p.

JUNG, S.; HOERNES, S.; MEZGER, K. Synorogenic melting of mafic lower crust: constraints from geochronology, petrology and Sr, Nd, Pb and O isotope geochemistry of quartz diorites (Damara orogen, Namibia). **Contributions to Mineralogy and Petrology**. n.143. 2002. p.551-566.

KOPRUBAS¸ N.; ALDANMAZ, E. Geochemical constraints on the petrogenesis of Cenozoic I-type granitoids in Northwestern Anatolia, Turkey: evidence for magma generation by lithospheric delamination in a post-collisional setting. **Int Geol Rev**. n. 46. 2004. p.705-729.

NACHIT, H.; IBHI, A.; ABIA, E. H.; BEN OHOUD, M. Discrimination between Primary magmatic biotites, reequilibrated biotites and neoformed biotites. **C. R. Geoscience**. n.337. 2005. p.1415-1420.

NEIVA, A. M. R. Geochemistry of hybrid granitoid rocks and of their biotites from Central Northern Portugal and their petrogenesis. **Lithos**. n.14. 1981. p.149-163.

PATIN˜ O DOUCE, A. E. Generation of metaluminous A-type granites by low-pressure melting of calc-alkaline granitoids. **Geology**. n.25. 1997. p.743-746.

PATIN˜ O DOUCE, A. E.; BEARD, J. S. Dehydration-meltingof biotite gneiss and quartz amphibolite from 3 to 15 kbar. **Journal of Petrology**. n.36. 1995. p.707-738.

PATIN˜ O DOUCE, A. E.; BEARD, J. S. Effects of P, F(O_2) and Mg/Fe ratio on dehydration meltingof model metagreywackes. **Journal of Petrology**. n.37. 1996. p.999-1024.

PATIN˜ O DOUCE, A. E.; MCCARTHY, T. C. Meltingof crustal rocks duringcontinental collision and subduction. In: HACKER, B. R.; LIOU J. G. (eds). **When Continents Collide**: geodynamics and geochemistry of ultrahigh-pressure rocks. Kluwer: Dordrecht. 1998. p.27–55.

PEARCE, J. A.; CANN, J. R. Tectonic setting of basic volcanic rocks investigated using trace element analyses. **Earth Planet Sci Lett**. n.19, 1973. p. 290-300.

PEARCE, J. A.; HARRIS, N. B. W.; TINDLE, A. G. Trace element discrimination diagrams for the tectonic interpretation of granitic rocks. Journal of Petrology. n.25. 1984. p. 956-983.

RAPP, R. O. Amphibole-out phase boundary in partially melted metabasalt, its control over liquid fraction and composition, and source permeability. **Journal of Geophysical Research**. n.100. 1995. p.15601-15610.

RAPP, R. P.; WATSON, E. B. Dehydration meltingof metabasalt at 8–32 kbar: implications for continental growth and crustmantle recycling. **Journal of Petrology**. n.36. 1995. p.891–931.

RASMUSSEN, K. L.; MORTENSEN, J. K. Magmatic petrogenesis and the evolution of (F:Cl:OH) fluid composition in barren and tungsten skarn-associated plutons using apatite and biotite compositions: case studies from the northern Canadian Cordillera. **Journal of Ore Geology Reviews**. n.50. 2013. p.118-142.

RUDNICK, R. L.; FOUNTAIN, D. M. Nature and composition of the continental crust: a lower crustal perspective. Reviews of Geophysics. n.33. 1995. p.267-309.

RUSHMER, T. Partial melting of two amphibolites: contrasting experimental results under fluid-absent conditions. **Contributions to Mineralogy and Petrology**. n.107. 1991. p.41–59.

SALEH, G. M.; DAWOOD, Y. H.; ABDEL-NABY, H. H. Petrological and geochemical constraints on the origin of the granitoid suite of the Homert Mikpid area, south Eastern Desert, Egypt. **Journal of Mineralogical and Petrological Sciences**. n.97. 2002. p.47–58.

SKJERLIE, K. P.; JOHNSTON, A. D. Vapour-absent meltingfrom 10 to 20 kbar of crustal rocks that contain multiple hydrous phases: implications for anatexis in the deep to very deep continental crust and active continental margins. **Journal of Petrology**. n.37. 1996. p.661-691.

STEVENS, G.; CLEMENS, J. D.; DROOP, G. T. R. Melt production duringg ranulite-facies anatexis: experimental data from 'primitive' metasedimentary protoliths. **Contrib Mineral Petrology**. n.128. 1997. p.352-370.

SPEER, J. A. **Mica in igneous rock**. In: MICAS BAILEY, S. W. eds. Mineralogical Society of America Review in Mineralogy. n.13. 1984. p.299-356.

SUDA, Y. Crustal anatexis evolution of granitoid magma in Permian intra-oceanic island arc, the Asago body of the Yakuno ophiolite, Southwest Japan. **Journal of Mineralogical and Petrological Sciences**. n.99. 2004. p.339-356.

TAYLOR, R. W. Phase equilibria in the system FeO-Fe_2O_3-TiO_2 at 1300°C. **Amer Mineral**. n.49. 1964. p.1016-1030.

TAYLOR, S. R.; McLENNAN, S. M. **The continental crust**: its composition and evolution, an examination of the geochemical record preserved in sedimentary rocks. Blackwell Scientific Publications: Oxford. 1985. 312 p.

VERHOOGEN, J. Distribution of titanium between silicates and oxides in igneous rocks. **Amer Jour Sci**. n.260. 1962a. p.211-220.

VERHOOGEN, J. Oxidation of iron-titanium oxides in igneous rocks. **Journal of Petrology**. n.70. 1962b. p.168-181.

VIELZEUF, D.; HOLLOWAY, J. R. Experimental determinations of fluid-absent meltingrelations in the pelitic system. **Contrib Mineral Petrology**. n.98. 1988. p.257-276.

WOLF, M. B.; WYLLIE, P. J. Dehydration-melting of solid amphibolite at 10 kbar: textural development, liquid interconnectivity and applications to the segregation of magmas. **Mineralogy and Petrology**. n.44. 1991. p.151-179.

WONES, D.R.; EUGESTER, H. P. Stability of biotite: Experiment, theory and application. **Amer Mineral**. n.50. 1965. p.1228-1272.

WYLLIE, P. J.; WOLF, M. B. Amphibolite-dehydration melting: sorting out the solidus. In: PRITCHARD, H. M.; ALABASTER, T.; HARRIS, N. B. W.; NEARY, C. R. (ed). Magmatic processes and plate tectonics. Special Publication n. 76: Geological Society of London. 1993. p. 405-416.